BUDOWNICTWO
CZASOPISMO TECHNICZNE
TECHNICAL TRANSACTIONS
CIVIL ENGINEERING
WYDAWNICTWO POLITECHNIKI KRAKOWSKIEJ
2-B/2010
ZESZYT 4
ROK 107
ISSUE 4
YEAR 107

BORIS BIELEK, MILAN BIELEK, DANIEL SZABÓ*

NEW KNOWLEDGE ABOUT REGIME OF NATURAL PHYSICAL CAVITY OF DOUBLE-SKIN TRANSPARENT FAÇADE UNDER WIND CLIMATE CONDITIONS – LONG TERM IN-SITU EXPERIMENTAL RESEARCH

NOWE INFORMACJE DOTYCZĄCE WARUNKÓW W NATURALNIE WENTYLOWANEJ SZCZELINIE PODWÓJNEJ FASADY TRANSPARENTNEJ PRZY WIETRZNYCH WARUNKACH KLIMATYCZNYCH – DŁUGOTRWAŁE BADANIA DOŚWIADCZALNE

Odpowiedzialność za poprawność językową ponoszą autorzy

Abstract

Formation of the theory of natural physical cavities based on the modern scientific disciplines: building solar thermal technology and aerodynamics of buildings or aerodynamics of cavities. Theory of natural physical cavities and its application references – double-skin transparent façades of intelligent buildings. Verification of the theory by application of long-term in-situ experiment. Experimental research of wind air flow through natural physical cavity of corridor type with year-round open circuit and with alternating air inlet and outlet modules. Description of the long-term experiment in-situ. Measured physical quantities: air temperatures of indoor and outdoor climate, characteristic air temperatures in the cavity, characteristic surface temperatures in the cavity, relative air humidity, intensity of global radiation. The velocity of air flow through the cavity.

Keywords: double-skin transparent façade, natural physical cavity, experiment in situ

Streszczenie

W artykule opisano teorię naturalnie wentylowanej szczeliny, wykorzystując nowoczesne dyscypliny naukowe. Przedstawioną teorię zastosowano w podwójnej fasadzie transparentnej budynku inteligentnego. Teorię zweryfikowano długotrwałymi badaniami doświadczalnymi *in situ*. Badania doświadczalne dotyczyły przepływu wiatru przez szczelinę wentylowaną typu korytarzowego z całorocznym otwartym obiegiem powietrza z alternatywnymi modułami wlotu i wylotu. Podczas badania mierzono właściwości fizyczne – temperaturę powietrza wewnętrznego i zewnętrznego, temperaturę powietrza w szczelinie, temperaturę na powierzchni szczeliny, wilgotność względną powietrza, intensywność promieniowania oraz prędkość przepływu powietrza przez szczelinę.

Słowa kluczowe: podwójna fasada transparentna, szczelina naturalnie wentylowana, badania in situ

* Doc. Ing. Boris Bielek, PhD.; Prof. Dr.h.c. Ing. Milan Bielek, DrSc; Mgr. Daniel Szabó, Department of Building Construction, Faculty of Civil Engineering, Slovak University of Technology.

Symbols

θ_a – air temperature [°C]
θ_s – surface temperature [°C]
φ_a – relative humidity of air [%]
v – air flow [m/s]
I_m – global solar radiation [W/m^2]
v_w – velocity of wind [m/s]
p_a – air pressure [Pa]

1. Introduction

Building of the Slovak National Bank in Bratislava was built in 1997–2002 (Fig. 1). Sustainable development program of the European building industry found response in its design and implementation to the ecological and energy efficient architectural-technical solution of intelligent buildings.

Fig. 1. View of the Slovak National Bank building in Bratislava

Rys. 1. Widok budynku Narodowego Słowackiego Banku w Bratysławie

2. Subject, goal and methodology of this paper

Subject of this paper is natural physical cavity (the dynamics of air flow – flow rate is based on natural convection and wind effect) of the double-skin transparent façade with corridor-type cavity (width = 600 mm), with interlaced function (inlet – outlet) of air distribution channels, with year-round open circuit and effective height equal to the height of one floor. Outer skin of the façade is glazed with single safety glazing system (Fig. 2).

Goal of this paper is the quantification of thermal, aerodynamic and energy regime of the natural physical cavity of the double-skin transparent façade.

Methodology of this paper is experiment in-situ. That means under the load of real conditions of the exterior climate on the building.

3. Experiment in-situ. Basic data, physical parameters, measuring technology

The experiment was carried out on 17th floor, 56.3 m above the terrain. Orientation of the experimentally examined part of the cavity was SW (240°). Duration of the experiment was 18 months (6 months test series, 12 months measurement).

We monitored the following physical parameters in the experiment (Fig. 2):

A. Temperature

- θ_{ae} – air temperature of the exterior climate [°C] (Fig. 4),
- θ_{ai} – air temperature of the interior climate [°C] (Fig. 4),
- $\theta_1 = \theta_{a,\mathrm{INLET}}$ – air temperature at inlet to the facade [°C],
- $\theta_2 = \theta_{a,\mathrm{OUTLET}}$ – air temperature at outlet from the facade [°C],
- $\theta_3 = \theta_{am,d1}$ – air temperature in the lower part of the cavity – inlet module [°C],
- $\theta_4 = \theta_{am,d2}$ – air temperature in the lower part of the cavity – outlet module [°C],
- $\theta_5 = \theta_{am,s1}$ – air temperature in the central part of the cavity – inlet module [°C] (Fig. 5),
- $\theta_6 = \theta_{am,s2}$ – air temperature in the central part of the cavity – outlet module [°C],
- $\theta_7 = \theta_{am,h1}$ – air temperature in the upper part of the cavity – inlet module [°C],
- $\theta_8 = \theta_{am,h2}$ – air temperature in the upper part of the cavity – outlet module [°C],
- $\theta_9 = \theta_{\mathrm{sim,OUT,1}}$ – temperature on the internal surface of the cavity – outer skin of the double-skin facade – inlet module [°C] (Fig. 6),
- $\theta_{10} = \theta_{\mathrm{sim,INT,1}}$ – temperature on the internal surface of the cavity – inner skin of the double-skin facade – inlet module [°C],
- $\theta_{11} = \theta_{\mathrm{sim,OUT,2}}$ – temperature on the internal surface of the cavity – outer skin of the double-skin facade – outlet module [°C],
- $\theta_{12} = \theta_{\mathrm{sim,INT,2}}$ – temperature on the internal surface of the cavity – inner skin of the double-skin facade – outlet module [°C],
- $\theta_{13} = \theta_{si,1}$ – temperature on the internal surface of the double-skin facade – inlet module [°C] (Fig. 6),
- $\theta_{14} = \theta_{si,2}$ – temperature on the internal surface of the double-skin facade – outlet module [°C].

B. Relative humidity

- φ_{ae} – relative humidity of the external climate air [%] (Fig. 4),
- φ_{ai} – relative humidity of the internal climate air [%] (Fig. 4).

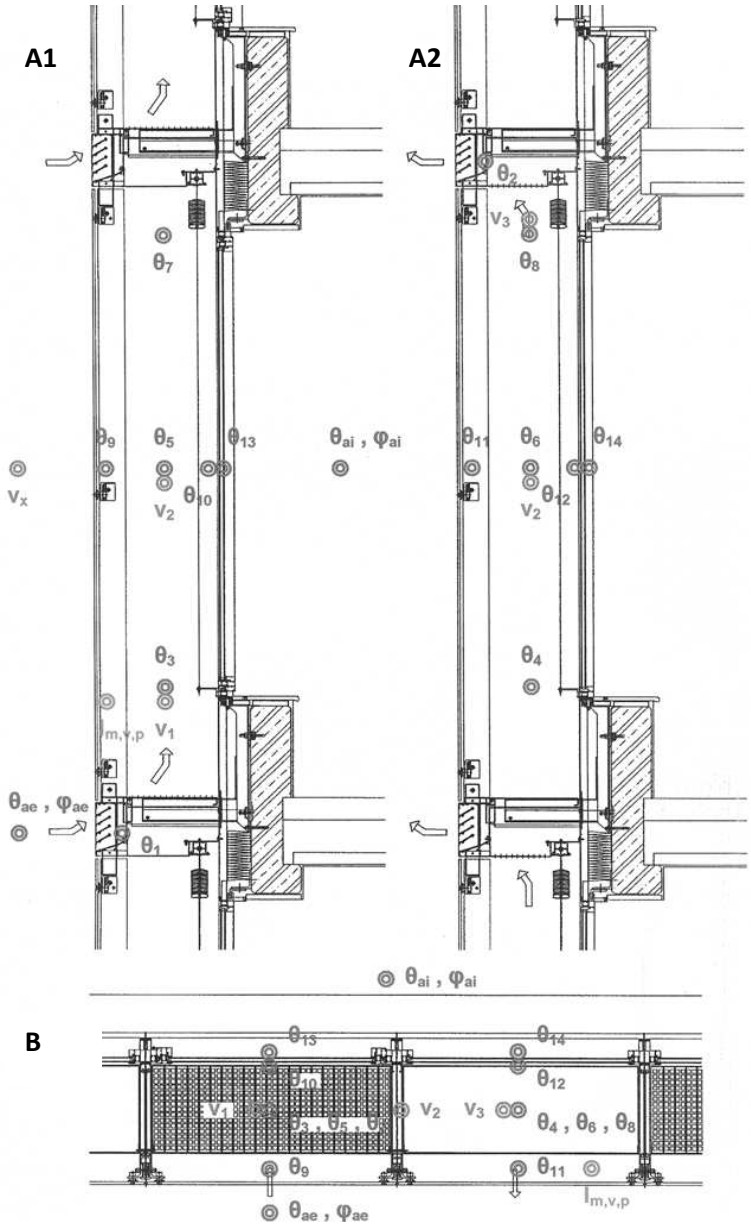

Fig. 2. Examined physical parameters of the double-skin transparent façade: A1 – vertical section – inlet module, A2 – vertical section – outlet module, B – horizontal section through inlet and outlet modules

Rys. 2. Parametry fizyczne badanej podwójnej transparentnej fasady: A1 – przekrój pionowy – moduł wlotowy, A2 – przekrój pionowy – moduł wylotowy, B – przekrój poziomy wzdłuż modułów wlotowego i wylotowego

Fig. 3. Data acquisition switch unit

Rys. 3. Akwizycja danych jednostki przełącznika

Fig. 4. Temperature and humidity convertor

Rys. 4. Czujnik do pomiaru temperatury i wilgotności

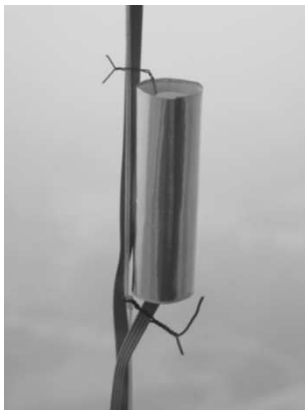

Fig. 5. Sheltered probe for air temperature measurement

Rys. 5. Osłonięty czujnik do pomiaru temperatury i wilgotności

Fig. 6. Probes for surface temperature measurement

Rys. 6. Sondy do pomiaru temperatury powierzchni

Fig. 7. Probes for air flow velocity measurement

Rys. 7. Sondy do pomiaru prędkości przepływu powietrza

Fig. 8. Solarimeter

Rys. 8. Solarymetr

C. Air flow

$v_1 = v_{m,d1}$ – air flow in the lower part of the cavity – inlet module [m·s^{-1}],

$v_2 = v_{m,s1-2}$ – air flow in the central part of the cavity on the boundary between inlet and outlet module [m·s^{-1}) (Fig. 7),

$v_3 = v_{m,h2}$ – air flow in the upper part of the cavity – outlet module [m·s^{-1}].

D. Solar radiation

$I_{m,v,\mathrm{SW}}$ – global solar radiation falling on vertical plane with SW aspect [W·m^{-2}],

$I_{m,v,p}$ – global solar radiation falling on vertical plane with SW aspect transmitted through the outer transparent skin [W·m^{-2}] (Fig. 8).

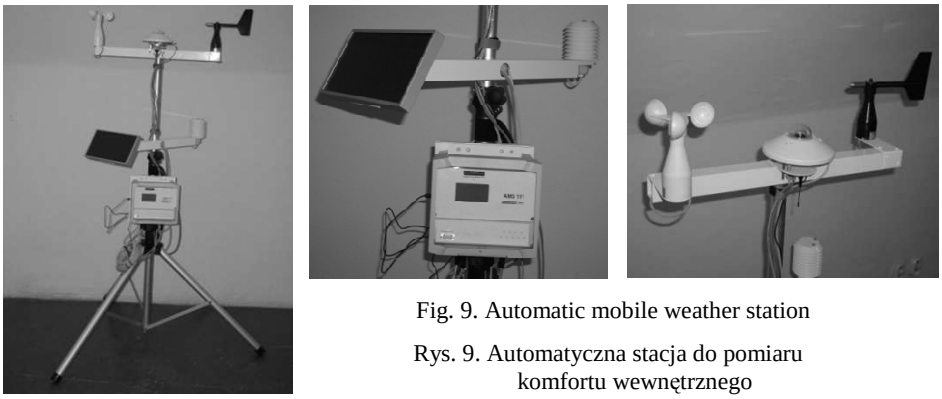

Fig. 9. Automatic mobile weather station

Rys. 9. Automatyczna stacja do pomiaru komfortu wewnętrznego

E. Wind

$v_{w,x}$ – wind velocity ($m \cdot s^{-1}$) and wind direction (N, NE, E, SE, S, SW, W, NW) (Fig. 9).

In the experiment in-situ, the above mentioned parameters (Fig. 2) were scanned and recorded:

- air temperature: θ_1, θ_2, θ_3, θ_4, θ_5, θ_6, θ_7, θ_8, θ_{ai}, θ_{ae}: by shielded sensors Pt 100 from HAYASHI DENKO Co. Ltd., Tokyo, Japan,
- surface temperature: θ_9, θ_{10}, θ_{11}, θ_{12}, θ_{13}, θ_{14}: by sensors Pt 100 from HAYASHI DENKO Co., Ltd., Tokyo, Japan,
- relative air humidity: φ_{ae}, φ_{ai}: by converters MWPA 12-3321423 from SENZORIKA s.r.o., Prague, Czech Republic,
- velocity of air flow: v_1, v_2, v_3: by converters EE61-VC5 from E+E Elektronik, Austria,
- global solar radiation: $I_{m,v,p}$, $I_{m,h}$: by pyranometers CM11 from KIPP&ZONEN B.V., the Netherlands,
- wind – velocity and direction: v, (N, NE, E, SE, S, SW, W, NW): by automatic mobile weather station IMS AMS 111 from MicroStep – MIS, Slovak Republic.

Continuous record of the scanned physical parameters was processed by data acquisition switch unit AGILENT 34970A from AGILENT TECHNOLOGIES, CA, USA.

4. The methodology of processing the experiment results

From the extensive long-term experimental examination of the physical regime of the cavity of the double-skin transparent façade, for the purpose of this paper, we selected only summer period (the highest energy efficiency) and that in the form of the typical situations – Table 1, Fig. 10. The determining inputs for their selection were:

- the global solar radiation falling on a vertical plane (SW) $I_{m,v,SW}$ [W/m^2],
- the global solar radiation (SW) transmitted through the outer transparent skin $I_{m,v,p}$ [W/m^2],
- the wind velocity $v_{w,x}$ [m/s] and its drection (N, NE, E, SE, S, SW, W, NW),
- the velocity of the air flow in the cavity:
  $v_1 \equiv v_{mA1}$ [m/s] in the lower part of the inlet module A1,
  $v_3 \equiv v_{mA2}$ [m/s' in the upper part of the outlet module A2 – Fig. 2.

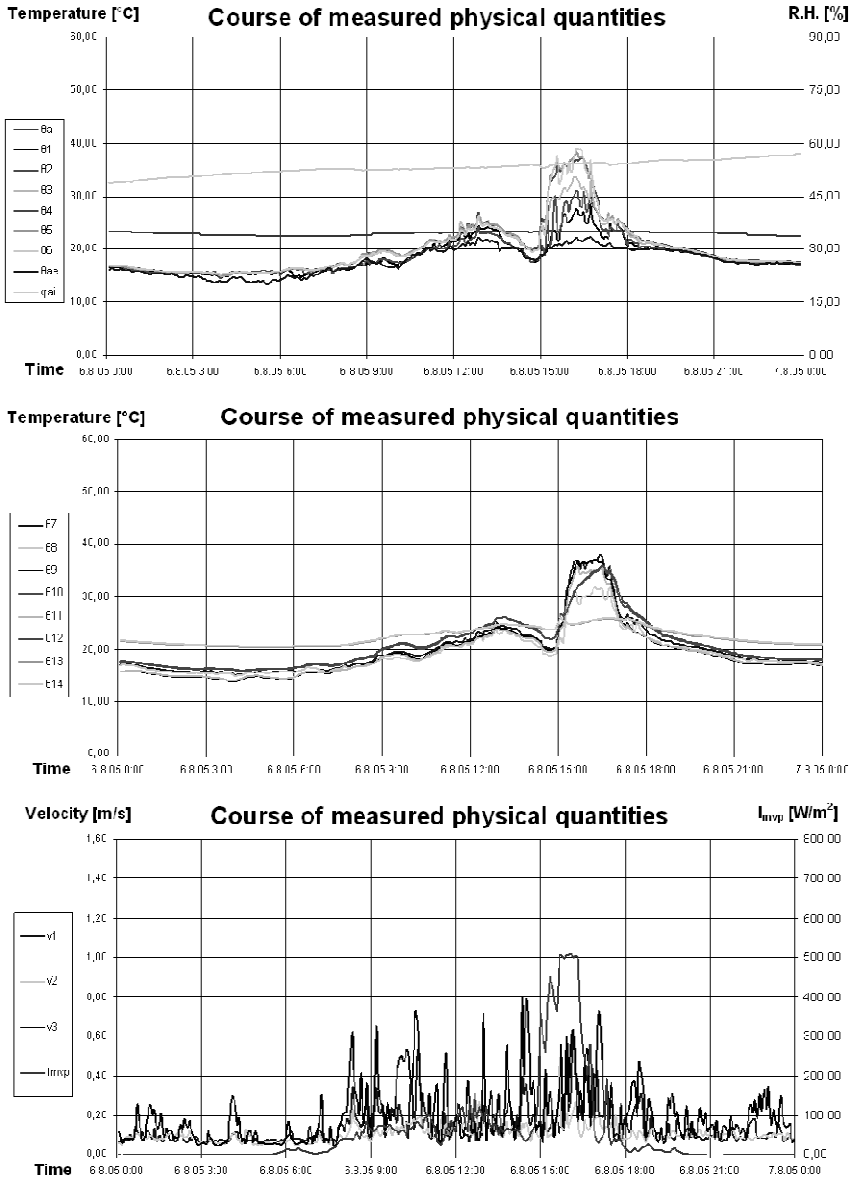

Time	θ_{ai}	ϕ_{si}	v_1	v_3	θ_1	θ_2	θ_3	θ_4	θ_5	θ_6	θ_7	θ_8	θ_{ae}	I_{mvp}
6.8.05 15:55	23,17	54,23	0,59	0,60	25,06	28,96	30,97	35,51	34,78	34,25	35,16	29,95	21,62	506,78

Fig. 10. The example of measured values from the experiment for the typical situation IV.B – Table 1

Rys. 10. Przykład zmierzonych wartości z doświadczenia dla typowej sytuacji – IV. B tabeli 1

Table 1

The concept for the typical situations connected with the selection of experimentally measured values of physical parameters characterizing the physical regime of the cavity during the effect of the wind ($v_{w,x}$ > 0,5 m/s)

Inputs for the selection of the parameters				Typical situation
$I_{m,v,p}$ [W/m^2]		v_1 or v_3 [m/s]		
I	0	A	0,2–0,4	I.A
		B	0,4–0,8	I.B
		C	0,8–1,2	I.C
II	0–200	A	0,2–0,4	II.A
		B	0,4–0,8	II.B
		C	0,8–1,2	II.C
III	200–400	A	0,2–0,4	III.A
		B	0,4–0,8	III.B
		C	0,8–1,2	III.C
IV	400–600	A	0,2–0,4	IV.A
		B	0,4–0,8	IV.B – Fig. 10
		C	0,8–1,2	IV.C

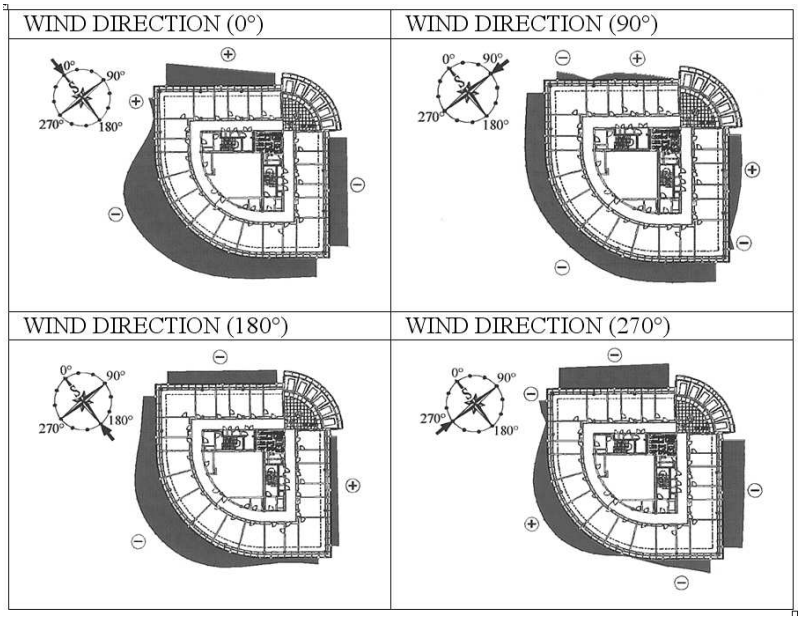

Fig. 11. The distribution of the aerodynamical coefficients of external pressure on the surfaces of the external walls of the double-skin transparent façade of the building of the Slovak National Bank in Bratislava for the selected wind directions. Altitude level of 17th floor, H = 56,3 m) [2]

Rys. 11. Podział aerodynamicznych współczynników ciśnienia zewnętrznego na powierzchnię ścian zewnętrznych podwójnych fasad transparentnych w budynku Słowackiego Banku Narodowego w Bratysławie ze względu na wybrane kierunki wiatru. Wysokość pomiaru – 17 piętro, H = 56,3 m) [2]

The aerodynamical coefficient of the external pressure on the building C_{pe} [–] is highly variable – Fig. 11. The air, because of the wind effect, enters into the geometrically defined cavity in principle by both openings (lower and upper). If the cavity is filled by air during the wind blast ($p_{ae} = p_{am}$ [Pa]), then the air in the cavity moves in the direction of the opening with the lower aerodynamical coefficient of external pressure (up or down direction).

In the subject methodology we therefore applied the higher from the velocities of air flow through the cavity (v_1 or v_3 [m/s]). This velocity of air flow through the cavity is a function of the velocity during the wind blast $v_{w,N}$ [m/s], the temperatures of the exterior climate θ_{ae} [°C], the aerodynamical coefficients of local resistances ξ_x [–] and the resistances of the friction along the length of air flow trajectory through the cavity, the effect of the global solar radiation $I_{m,v,SW}$ [W/m^2] and the conditions of natural convection. Theoretical expression of the relation between the velocity during the wind blast $v_{w,N}$ [m/s] and the velocity of air flow in the cavity v_1 or v_3 [m/s] is highly demanding and therefore it is preferable to determine this relation experimentally.

5. The results of the experiment

From the sequence of measured values of the examined physical parameters we can observe that:

- Interaction between the air temperature of the exterior climate θ_{ae} [°C] and the thermal comfort temperature θ_{ai} [°C] for office work in light to medium dress corresponds with the designed climatic and energy concept of the building. For $26 \leq \theta_{ae}$ [°C] ≤ 32 the temperature of the interior climate is in the range $22 \leq \theta_{ai}$ [°C] ≤ 27.
- If the exterior climate is characterized by the absence of the global solar radiation $I_{m,v} = 0$ [W/m^2] or during the dark hours of the day, the maximum and also the average air temperature in the cavity during the wind effect ($v_w > 0{,}5$ m/s) is equal to the temperature of the exterior climate $\theta_{am} \approx \theta_{ae}$ [°C].
- If the exterior climate is characterized by the effect of the global solar radiation $I_{m,v} \neq 0$ [W/m^2], then the increase of its value also increases the air temperature in the cavity max θ_{am} [°C] and avg θ_{am} [°C] during the effect of the wind – Fig. 12.
- The increase of the air temperature in the cavity $\Delta\theta_{am} = \theta_{am} - \theta_{ae}$ [K] is not linear as it is assumed by the actual theoretical calculations – Fig. 13.
- The highest increase of the air temperature in the cavity max $\Delta\theta_{am}$ [K] during the wind effect is approximately in the middle of its effective height. The second highest increase of the air temperature in the cavity $\Delta\theta_{am}$ [K] during the wind effect is approximately in one sixth of the upper part of the effective height.
- Even if the effect of the wind blast "flushes" the air through the whole cavity, still there is a sign of stagnation of air of higher temperatures in the upper part of the inlet module and in the lower part of the outlet module – Fig. 13, Fig. 14.
- During the effect of the wind the values of the maximum air temperature in the cavity max θ_{am} [°C] are from 1 to 4 K higher than the average air temperatures in the cavity avg θ_{am} [°C].
- Considering the pattern of the increase of the air temperatures in the cavity during the wind effect (Fig. 13) in the inlet and outlet module, the centroidal temperature can be found approximately in the halfway of the effective height $H/2$ [m].

– Considering the dynamics of the air motion in the cavity during the effect of the wind blasts it is correct to express its temperature by the average value avg θ_{am} [°C] (Fig. 13, Fig. 14) and also utilize it for the quantification of the heat demand for natural ventilation from the cavity.
– The processing of the typical situations from the long term experimental measurement (Table 1, Fig. 10) to the level which is represented by Fig. 13 and Fig. 14 allows to plot the graphical dependance of the average air temperature in the cavity avg θ_{am} [°C] from the effect of the global solar radiation $I_{m,v,p}$ [W/m^2] and the effect of the wind $v_{w,N}$ [m/s], which creates air flow motion in the cavity $v_{1,3}$ [m/s] – Fig. 12.

$$aver\ \theta_{am} = \frac{\sum_{x=3}^{8} \theta_{amx}}{6}\ (^{o}C)$$

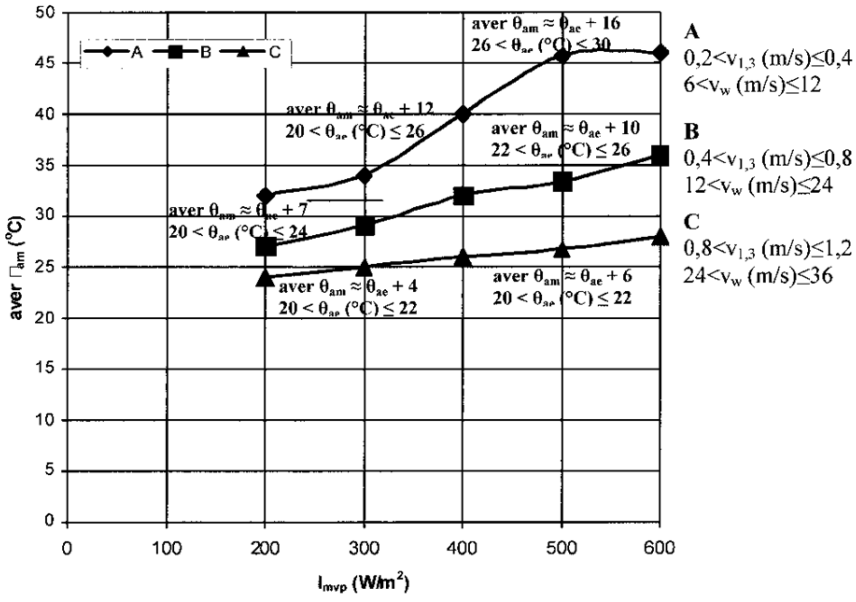

I.	II.	III.	IV.
I_{mvp}=0 W/m^2	0<I_{mvp} (W/m^2)≤200	200<I_{mvp} (W/m^2)≤400	400<I_{mvp} (W/m^2)≤600
aver θ_{am}≈ θ_{ae} (°C)	aver θ_{am}≈ θ_{ae}+2 (°C)	aver θ_{am}=f(v_w) (°C) aver θ_{am}=f($v_{1,3}$) (°C)	aver θ_{am}=f(v_w) (°C) aver θ_{am}=f($v_{1,3}$) (°C)

Fig. 12. Dependence of the average air temperature in the cavity avg θ_{am} [°C] from the effect of the global solar radiation $I_{m,v,p}$ [W/m^2] and the wind effect $v_{w,N}$ [m/s] or the air flow motion in the cavity $v_{1,3}$ [m/s]

Rys. 12. Zależność średniej temperatury powietrza w pustce powietrznej avg θ_{am} [°C] od skutków całkowitego promieniowania słonecznego $I_{m,v,p}$ [W/m^2] oraz efektu wiatru $v_{w,N}$ [m/s] lub ruchu powietrza w pustce $v_{1,3}$ [m/s]

– In general, it is needful to state that the experimentally acquired average and maximum increase of the air temperature in the cavity as a function of the effect of the global solar radiation and the effect of the wind have higher values of avg $\Delta\theta_{am} \approx 19$ K, max $\Delta\theta_{am} \approx 22$ K (Fig. 14) than they were determined by the theoretical calculation of the value max $\Delta\theta_{am} \approx 10$ K [2].

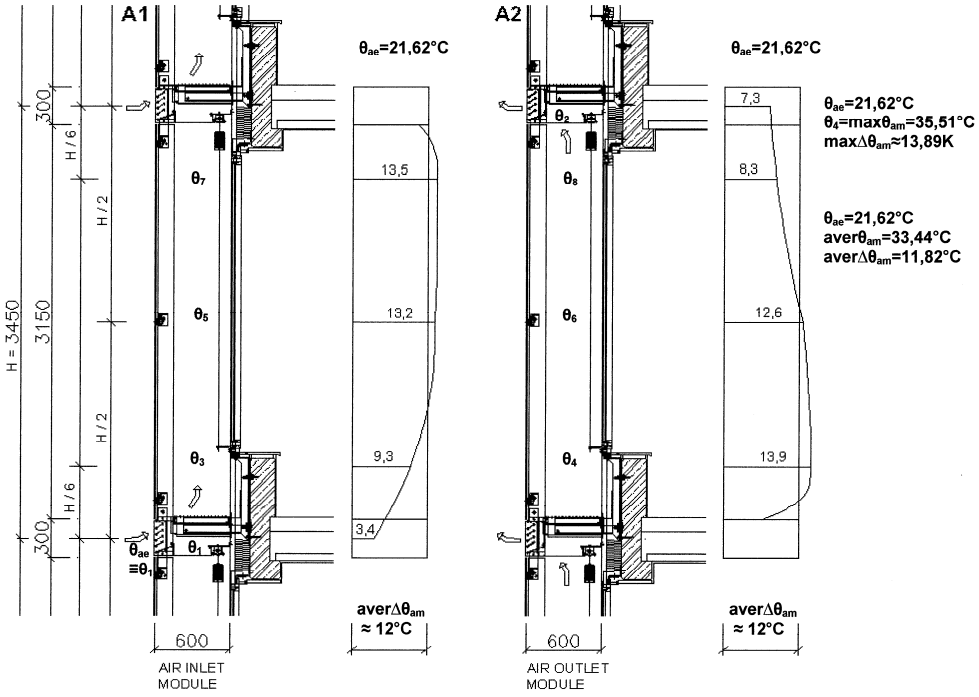

Fig. 13. Typical increase of the air temperature in the natural physical cavity of the double-skin transparent façade during the effect of the wind. Typical situation IV.B – Table 1, Fig. 10; A1 – inlet module of the cavity, A2 – outlet module of the cavity – Fig. 2

Rys. 13. Typowy wzrost temperatury powietrza w naturalnej pustce powietrznej podwójnej fasady transparentnej spowodowany działaniem wiatru. Typowa sytuacja IV.B, tabela 1, rys. 10; A1 – moduł wlotowy pustki, A2 – moduł wylotowy pustki, rys. 2

– The values of the increase of temperatures in the natural physical cavity that are acquired by the experiment during the comparable load by the effect of the global solar radiation $I_m \approx 600$ W/m^2 and during the effect of the wind are approximately double in value than by the theoretical calculation. This is the most significant knowledge from the long term experiment in the field of climatic load on the cavity during the effect of the wind.

6. Conclusions

The new knowledge about the physical regime of the natural physical cavity under the windless climate conditions acquired by the experimental in-situ research are important and useful in the following fields:

– formation and development of the theory of natural physical cavities with application of new façade technology of buildings,
– design of the dynamic simulation software for the calculation experiments of energy regimes of natural physical cavities,
– design of etalons for fine-tuning of the existing numerical calculation software for this climate dependent problem,
– confrontation of the existing models of outdoor climate in the form of test reference years of a specific locality with the condition of the real climate.

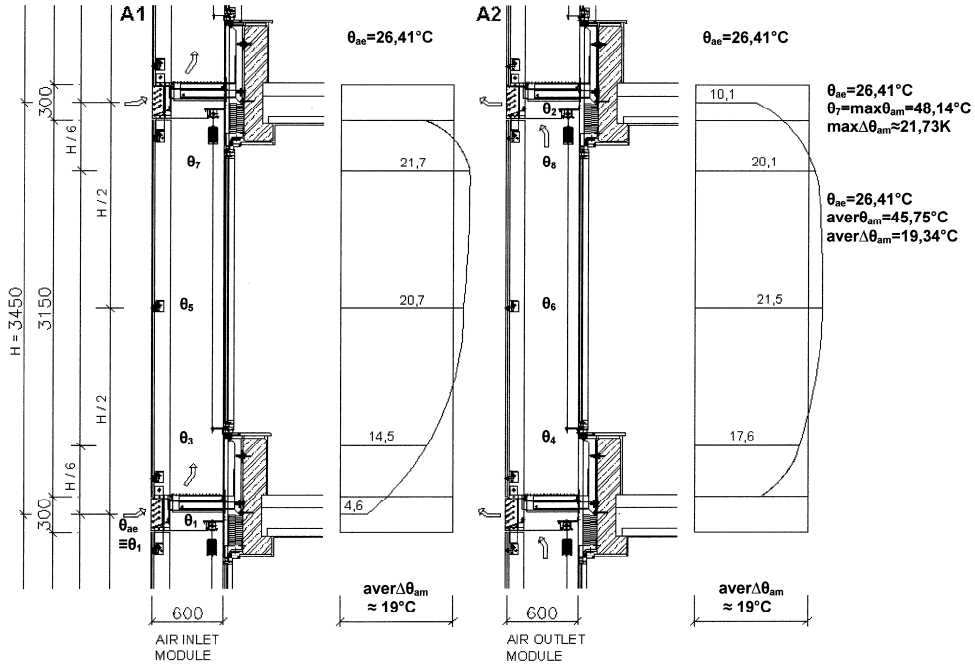

Fig. 14. Typical increase of the air temperature in the natural physical cavity of the double-skin transparent façade during the effect of the wind. Typical situation IV.A – Table 1, Fig. 10; A1 – inlet module of the cavity, A2 – outlet module of the cavity – Fig. 2

Rys. 14. Typowy przyrost temperatury powietrza w pustce powietrznej podwójnej fasady transparentnej spowodowany działaniem wiatru. Typowa sytuacja IV.B, tabela 1, rys. 10 A1 – moduł wlotowy pustki, A2 – moduł wylotowy pustki, rys. 2

References

[1] Bielek M., Bielek B., Szabó D., *Physical cavity of double-skin façade – experiment in-situ*, [in:] CESB 07 Prague Conference Central Europe towards Sustainable Building, Proceedings, Vol. 2, CBS Servis, s.r.o., Prague 2007, 445-450.
[2] Bielek B., Bielek M., Kusý M., Paňák P., *Dvojité transparentné fasády budov. 2. diel: Vývoj, simulácia, experiment a konštrukčná tvorba fasády budovy NBS v Bratislave*, Coreal, spol. s r.o., Bratislava 2002.
[3] Bielek B., Bielek M., Palko M., *Dvojité transparentné fasády budov. 1. diel: História, vývoj, klasifikácia a teória konštrukčnej tvorby*, Coreal, spol. s r.o., Bratislava 2002.

This work was supported by the Scientific Grant Agency of the Ministry of Education of Slovak Republic and Slovak Academy of Sciences in the project VEGA 1/0316/09.